Summer 8-19-2022

Immiscible Liquid-infused Filters for Water and Aerosol Filtration

Justin Hardcastle
University of Maine, justin.hardcastle@maine.edu

IMMISCIBLE LIQUID-INFUSED FILTERS FOR WATER AND AEROSOL FILTRATION

By

Justin Hardcastle

B.S. University of New Hampshire, 2020

A THESIS

Submitted in Partial Fulfillment of the

Requirements for the Degree of

Master of Science

(in Biomedical Engineering)

The Graduate School

The University of Maine

August 2022

Advisory Committee:

Caitlin Howell, MS, Ph.D, Associate Professor of Biomedical Engineering

Sue Ishaq, Ph.D, Assistant Professor of Animal and Veterinary Science

Richard Corey, MFA, Ph.D, Director of the VEMI Lab

IMMISCIBLE LIQUID-INFUSED FILTERS FOR WATER AND AEROSOL FILTRATION

By Justin Hardcastle

Thesis Advisor: Dr. Caitlin Howell

An Abstract of the Thesis Presented
in Partial Fulfillment of the Requirements for the
Degree of Master of Science
(in Biomedical Engineering)
August 2022

In the purification of water and air, membrane fouling is an ongoing issue that leads to the reduction of filter efficiency over time. An increase in the frequency of current chemical and mechanical cleaning methods increases system downtime, increases overall costs, and leads to the reduction of the lifetime of the membrane. Commonly used filtration materials such as polytetrafluorethylene (PTFE) and polyvinylidene fluoride (PVDF) are porous throughout and have a textured surface that facilitates the adhesion of bacteria and other foulants. To prevent this adhesion, bioinspired liquid-coated filters are proposed as a new approach to creating filters that resist fouling. Liquid-coated filters were created by immobilizing a water-immiscible liquid on the surface of commercially available synthetic filters. For water filtration tests, 0.45 μm pore diameter PTFE and PVDF filters were coated with omniphobic perfluoropolyether (PFPE) liquids. The continuity of the surface liquid layer was measured by testing how easily a water droplet could begin to move on the surface. The results indicate that infused PTFE membranes form a superhydrophobic surface with a sliding angle of approximately 5°, 75% lower than the infused PVDF. The ability of the infused membranes to resist biofilm formation was measured by incubating in growth media with *Staphylococcus epidermidis* for 24 hours. Infused PVDF membranes reduced biofilm formation by approximately 25% compared to bare controls while infused PTFE membranes reduced biofilm formation by approximately 98%. Pure water

permeability (PWP) experiments conducted at an applied pressure of 1.5 bar indicated that liquid-coated PVDF membranes had a statistically equivalent PWP of 2827 ± 323 L/m^2-h-bar, for over 10 cycles of use, showing that the immobilized liquid is present and stable within the pores. For aerosol filtration materials, new solid-liquid pairings were investigated. HEPA filters were infused with PFPE and evaluated for their ability to resist crystal violet staining and the changes in filtration efficiency. Infused HEPA filters showed an increased ability to resist crystal violet staining, but a lowered filtration efficiency. The fouling resistance of the infused HEPA filters suggest that sample viability after recovery could be increased and that these filtration materials could be applied to an air sampling system for public health monitoring. Based on the positive results of both liquid-coated PVDF and HEPA filters in functional applications despite poor results in surface characterization, we've begun exploring how to create more sustainable liquid-coated filters. Paper filters were coated with a thin layer of polydimethylsiloxane (PDMS) via chemical vapor deposition. These PDMS-coated paper filters were then infused with silicone oil. These new liquid-coated paper filters will be characterized based on surface properties and for functionality with aerosol and liquid filtration. The use of liquid-coated materials in water and air purification applications opens new doors for the creation of filtration materials that resist the adhesion of contaminants and resist fouling.

ACKNOWLEDGEMENTS

I want to thank all of my friends and family who supported me throughout the years. They were the ones who were always there for me no matter how dark things became, the ones who helped me pull myself out of the depths. Not only could I have not done this without them, but there's no way I'd be here without their love and support. From the bottom of my heart, thank you.

TABLE OF CONTENTS

LIST OF FIGURES

CHAPTER 1

INTRODUCTION

According to the World Health Organization (WHO), 1 in 9 people do not have access to clean water[1,2]. Approximately 1.9 billion people are still reliant on potentially contaminated or an unimproved source of drinking water[2]. Many waterborne infections result in diarrhea and the loss of bodily fluids which can lead to dehydration and death. For children under the age of 5, diarrhea is the fifth leading cause of death[3]. Approximately 88% of diarrhea associated deaths are directly linked to unsafe water, poor sanitation, and insufficient hygiene[2,3]. Water filtration is an essential process to human health for the production of clean water for drinking, medical, and pharmaceutical applications.

Water filtration removes or reduces the concentration of particulate matter in solution, such as suspended particles, microbes, viruses, and other undesirable chemical and biological contaminants[4]. Filtration is performed through the use of filters or membranes to separate particles based on specific properties such as size or charge[5]. Membranes have been used in solid-liquid separation devices for many years in biological treatment and physical applications[6]. These membranes are characterized based on pore size, type of material used, and application[5]. Membrane water filters have a three dimensional (3D) porous structure and can be divided into four types based on filtration media and pore size: reverse osmosis (RO), nanofiltration (NF), ultrafiltration (UF), and microfiltration (MF)[1]. Ultrafiltration systems are cost-effective for operation due to low energy consumption, are simple to scale up, and have excellent chemical and thermal stability with a long service life. These systems are ideal for removing suspended matter, bacteria, and some viruses[7].

The advancement of membrane science has greatly driven the improvement of water filtration technology, yet due to population increase and environmental concerns, the need for novel methods for water purification remains a global issue[4]. There are two main challenges that membrane technology needs to address. The first challenge is creating new materials that can be used for more cost-effective membranes that are more durable, inexpensive, and with fewer environmental concerns[4]. The second challenge is to develop novel methods to prevent loss of filter efficiency.

Materials in Water Filtration

Creating efficient filters is essential to environmental health, human health, manufacturing, and healthcare. An efficient filter has high permeation flux, high retention, and a low pressure drop[4]. Over time, these materials can lose efficiency as they build up contaminants that have been removed from solution. The membrane being used for separation processes is constantly in contact with the solution that is being treated, and is therefore prone to the deposition and buildup of chemical and biological matter[8]. The buildup of contaminants, known as membrane fouling, is one of the main issues that leads to the reduction of process productivity and membrane lifetime[9]. Four main mechanisms of fouling in pressure driven membrane processes (complete pore blocking, partial pore blocking, internal pore blocking, and cake formation)[8]. In order to address these mechanisms of fouling, the nature of the foulants must be considered (organic, inorganic, or biological)[8]. These mechanisms can involve adsorption, accumulation, or precipitation either on the surface or within the pores of the membrane[8,9].

Fouling behavior and characteristics vary based on filtration modes (relaxation, backwash, mixed, and continuous). The distribution of proteins and carbohydrates can vary in membranes of bioreactors between internal and external fouling and the operating conditions[10]. Current methods

for cleaning fouled membranes and filters involve removing the foulant by chemical or physical cleaning methods[11–13]. Physical methods can include using ultrasound frequencies, electric fields, alternating flow patterns, and more[12]. Physical methods require many factors to be considered before being chosen, since they can affect different materials and systems differently. Polyvinylidene fluoride (PVDF) for example, is more resistant to ultrasound waves than polyethersulfone (PES)[12]. Chemical cleaning methods can include the use of alkaline solutions, metal chelating agents, or surfactants[11]. Alkaline solutions are best suited for removing organic foulants from membranes by hydrolysis and the solubilization of the fouling layer[11,13]. Metal chelating agents are used to remove divalent cations from the complexed organic molecules and can weaken the structure of the fouling layer matrices[11]. Surfactants are used to solubilize the foulants by forming micelles around the less soluble macromolecules and help remove them from the membrane surface[11,14]. Different foulants will respond differently based on what type of chemical method is used for removal. This may require a more detailed knowledge about the foulant type to address the fouling issue, and the use of chemical cleaning agents will add to the ongoing price of operation for a filtration system.

Membrane Fouling

Fouling, modeling and wastewater treatment are the dominant research areas for ultrafiltration membranes, making up 27%, 17% and 12% of publication output respectfully[15]. Carbon-based materials (biochar, carbon nanotubes, graphene, mesoporous carbon nanoparticles, and carbon quantum dots) show promise in developing novel and high-performance membranes for filtration[16].

Fouling of membranes with biological material can lead deposition and growth of unwanted biofilms, known as biofouling, and can occur in a wide variety of situations and

environments[9]. This phenomenon occurs on large scales such as the fouling of ship hulls and pipelines, and on smaller scales such as the colonization of biomedical devices and in filtration systems for drinking water[17]. Biofouling reduces membrane flux and reduces the life of the membrane[16]. Bioadhesion is the first step in biofilm formation, and is driven by a variety of nonspecific interactions, such as long-range electrostatic forces, hydrophobic forces, van der Waals, hydrogen bond interactions[18]. Due to the self-replicating nature of bacteria, any form of sterilization that is less than 100% effective can lead to contamination and biofouling. The remains of dead bacteria are an ample food source for any surviving bacteria. Membrane biofouling is affected by a wide range of factors, such as shear, pressure, characteristics of the bacteria, the membrane surface, environmental factors (pH, ionic strength, ion species). Polymeric membranes are often hydrophobic, and allow for the adhesion of non-polar solutes, hydrophobic particles and bacteria[19].

Hydrophobic surfaces can be used for preventing the adhesion of hydrophilic foulants. Micropatterned surfaces can be built on top of microscopic pillars and the resulting effect is a superhydrophobic surface[20]. These types of surfaces gained attention for their potential applications in nanotechnology and in anti-fouling surfaces, but have some gaps that would need to be addressed before being applied to filtration systems[20]. One such challenge is that these systems can switch between the Cassie wetting state and the Wenzel wetting state based on changing conditions. The Cassie wetting state is when there is a composite interface with air pockets trapped under the droplet, making the surface display hydrophobic properties[20]. The surface can switch to the Wenzel wetting state, which is complete wetting of the surface, when the environmental conditions change outside of their normal range, such as increased temperature or pressure[20]. This transition makes these materials less ideal for filtration and purification

applications because of the specific requirements needed for operation. Impurities and a pressure driven process in the feed could easily disrupt these types of surfaces[20,21].

Bio-Inspired Filtration Solutions

In nature, the *Nepenthes* pitcher plant has evolved to use a specialized leaf design to capture insects for prey. A fully wettable water-lubricated anisotropic surface is created which forms an ultra-slippery surface that causes insect aquaplaning[22]. This causes the insects to fall into the pitcher portion of the plant to be digested. This design has been mimicked by scientists and engineers to create slippery liquid-infused porous surfaces (SLIPS)[23–25]. SLIPS are created by immobilizing liquid layers onto the surface of highly wettable microstructures which creates an omniphobic coating on solid surfaces that resists biofouling by preventing bacterial adhesion[24–26]. SLIPS have been shown to resist the adhesion of a variety of contaminants such as bacteria, blood, proteins, and crude oil[25–30]. These types of surfaces can be created on existing materials that already display the needed micro-nano porous structure[31]. This allows these materials to be expanded into new applications in engineering without being restricted to specific substrates.

Liquid layers have been developed on existing filtration materials to create liquid-based gated mechanisms that allow for multiphase selectivity[23,29,32]. These surfaces have demonstrated nonwetting properties that are caused by the immobilized immiscible liquid[32]. Surfaces that are hydrophobic due microstructures and stable air pockets are forced to rely on a stable air-liquid interface that prevents the surface from switching between the Cassie and the Wenzel wetting states. The use of immobilized liquid layers instead of trapped air pockets is able to overcome that challenge because the liquid is stabilized via capillary action[32]. Liquid-gated pores allow for a membrane to switch between two states based on a critical transmembrane pressure[23,29,32]. When the system is below the critical pressure, the immobilized liquid forms a uniform liquid layer and

seals the pores of the membrane. Above the critical pressure, the immobilized liquid is forced out of the way, and fluid is allowed to flow through the pore. When the pressure is released, the liquid layer reforms the uniform liquid surface[23,29]. These liquid gated-membranes have been reported to resist biofouling and allow for tunable multiphase selectivity for air-water-oil systems[23,29,33]

In this work, immobilized liquid layers are applied to existing filtration materials. This is done to improve resistance to biofouling, improve foulant recovery and prevent the buildup of contaminants. Water filtration applications are investigated for resistance to biofouling from bacteria. Aerosol filtration applications are investigated for resistance to the buildup of contaminants and for bacterial recovery. New sustainable membranes are investigated for both water and aerosol filtration applications.

CHAPTER 2: PTFE/PVDF MEMBRANES FOR WATER FILTRATION

Note: Portions of this chapter have been previously published in

ACS Appl. Mater. Interfaces 2022, 14, 6148−6156 by Rushabh M. Shah, Aydın Cihanoğlu, Justin Hardcastle, Caitlin Howell, and Jessica D. Schiffman

Background

Polyvinylidene fluoride (PVDF) and polytetrafluoroethylene (PTFE) are two common materials for water filtration. These materials are fluorinated and are hydrophobic in nature. In order to mimic the immobilized liquid layer of the *Nepenthes* pitcher plant, a fluorinated liquid phase must be used to match the fluorine chemistry of the materials. Previous studies have shown that these materials can be paired with a perfluoropolyether to create an immobilized liquid layer and an infused membrane that is ultra-slippery and resists biofouling[25,27,29,30]. PTFE is more fluorinated than PVDF and has better chemical matching at the molecular level with perfluoropolyether. PTFE is more hydrophobic than PVDF as well, but in turn is much more expensive. PTFE can be purchased for approximately \$0.70/cm^2, while PVDF can be purchased for approximately \$0.05/cm^2.[34] PTFE has been shown to be able to support liquid layers in previous studies as a super hydrophobic surface that resists bacterial fouling[23,25,35]. Krytox 103 (K103) is a perfluoropolyether. This fluorinated oil us used as a general-purpose oil that is used as a lubricant in the automotive industry[36]. It is clear, colorless, non-reactive, and stable under a wide variety of operating conditions including temperature ranges of -60 to 154°C[36]. Due to compatible fluorine chemistries, PTFE has a high affinity for K103, which allows it to be used to support an immobilized liquid layer[23,27,35]. PVDF has approximately half the number of fluorine atoms in each monomer when compared to PTFE, but is investigated for the support of liquid layers to reduce biofouling.

Filter Preparation

Poly (vinylidene fluoride) (PVDF) membranes were prepared by cutting 25mm diameter discs out of a 0.45 µm pore size PVDF sheet (ThermoFisher Scientific). These membranes were then soaked in 70% isopropyl alcohol for 30 minutes, washed three times with DI water and then stored in DI water for 24 hours. The membranes were allowed to dry in air until visually dry. PVDF membranes at this stage were used as dry controls. To create infused PVDF membranes, 30 µL of K103 (Perfluoropolyether Krytox 103, Dupont) was added dropwise to each membrane (6 $\mu L/cm^2$) and spread to coat the entire surface by tilting. Infused membranes were allowed to sit for 30 minutes horizontal, and then 1 hour vertical to drain the excess[27].

Polytetrafluoroethylene (PTFE) membranes with a pore size of 0.45 µm and a 25 mm diameter were purchased from Sterlitech. These membranes were used as purchased as dry controls. To make infused samples, 90 µL of K103 was added dropwise and spread by tilting.

Surface Characterization

Contact angle measurements are taken by placing a 10 µL droplet of DI water on the surface of the sample. Three different locations for each sample are tested for the contact angle. The droplets are photographed using a Canon Eos 6D Mark II camera with a 100 mm Macro lens from the side view. The images are processed using the Contact angle plugin for ImageJ using manual points selection. Two points are chosen along the base of the droplet, and then three points are chosen along the droplet edge.

Tilt angle measurements are performed by placing the sample on an AP180-Adjustable Angle Mounting Plate (Thorlabs, Newton, NJ) equipped with an AccuMaster digital level/angle gauge (Carson, NV). A 25 µL droplet of DI water is placed on one side of the sample, making sure

that the droplet is clear from the edge of the membrane to prevent edge effects. The stage is slowly tilted until the water droplet starts to move. The tilt angle measurement is recorded at the angle of inclination where there is consistent droplet movement, shown in **Figure 2A**. Each sample is tested 3 times, with the membrane being rotated approximately a quarter turn between measurements to ensure a new droplet path occurs each time. If no droplet movement occurs before 45°, the measurement is marked as a failure.

Biofilm Assay

A biofilm assay was performed by submerging samples in biofilm inducing media in a petri dish. Eight types of samples were created. Dry controls of PVDF and PTFE were made, some were submerged in only media, some were submerged with media that was inoculated with 70µL of *Staphylococcus epidermidis* stock culture. Liquid-infused samples of PVDF and PTFE were also created and submerged in media only wells and in inoculated media wells. These prepared samples were then incubated at 37°C without shaking for 24 hours. If samples floated when placed in the media, they were weighed down by ceramic weights so that they were completely submerged by the media. After incubation, the samples were carefully removed from the media and placed into a 0.01% crystal violet solution for 10 minutes. The samples were then removed from the crystal violet, washed gently twice in DI water, and then imaged with controlled lighting. The crystal violet in the samples was then extracted with a set amount of ethanol and the extracts were analyzed with a spectrophotometer by measuring the absorbance at 600 nm. These values were then normalized based on the absorbance of pure ethanol at 600 nm.

Filter Characterization

Professor Jessica Schiffman and her student, Rushabh Shah, at the University of Massachusetts at Amherst collaborated to investigate PVDF membranes to evaluate the performance of infused

PVDF membranes in a dead-end pure water permeability test[27]. This was done to measure the permeance of the membranes over repeated cycles. Pure water permeance tests were conducted using a 10 mL dead-end stirred cell (Sterlitech) that was pressurized with a nitrogen tank[27]. Flux was calculated by measuring the change of mass on the permeate side using a digital scale (U.S. Solid). Pressure values reported were gauge pressure values. Each bare membrane was compacted at 3 bar pressure for 0.5 h. Ten filtration cycles were performed (30 minutes each) on the same infused membrane sample at 1.5 bar transmembrane pressure with no resting time between cycles.

Results and Discussion

Contact angle measurements were taken of PVDF and PTFE samples to show that PTFE is more hydrophobic. Dry PTFE membranes show a higher contact angle of around 128±5.9°, while dry PVDF membranes show a contact angle of around 121±4.6°. **Figure 1** shows that these values are not statistically different, but PTFE is still slightly more hydrophobic. Contact angle measurements cannot be taken from infused samples because the presence of the oil layer causes a wrapping effect around the water droplet, changing the shape. This prevents an accurate measurement for contact angles from being taken.

To characterize the surface of infused membranes, tilt angle measurements were taken. This is done to show how easily a water droplet begins to slide off of the surface based on an incline. The angle is slowly increased until either the water droplet begins to show consistent

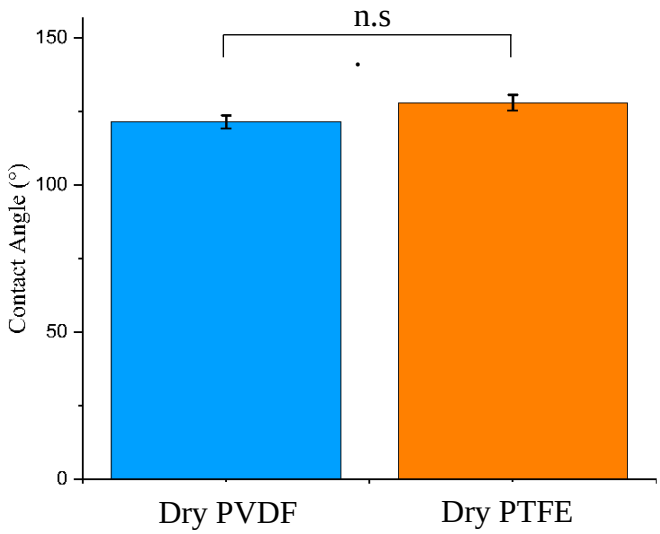

Figure 1: Contact angle of dry PVDF membranes and dry PTFE membranes. A Tukey test shows that samples are not statistically different.

movement, or no movement is seen before 45°. If no movement is seen before 45°, the trial is marked as a failure. Dry PVDF membranes show no droplet movement, and all trials were marked as failures. This shows that the water droplet was pinned in place, despite the surface being hydrophobic. PVDF membranes that were infused with K103 had a mixture of both failures and some successful tilt angle measurements. Shown in **Figure 2**, the average tilt angle for the infused PVDF membranes was 39.4±9.2°, but the results were highly variable and not statistically different from the dry PVDF membranes. This is a high tilt angle, meaning that the liquid layer is not well formed or that the liquid is easily pushed out the way by the water droplets. Dry PTFE membranes had a lower tilt angle than any of the PVDF membranes, with an average tilt angle of 29.4±5.1°. Infused PTFE membranes displayed an ultra-slippery surface (a surface with a tilt angle of lower than 10°) with an average tilt angle of 5.4±1.7°, which is significantly lower than any other sample

type ($p \leq 0.001$). This shows that the liquid layer is well formed and allows the water droplets to easily slide off the surface of the liquid layer.

Pure water permeability tests performed by Rushabh Shah at the University of Massachusetts Amherst of infused PVDF membranes over 10 consecutive filtration cycles shows that no significant change in permeance takes place. Two different infusing liquids were

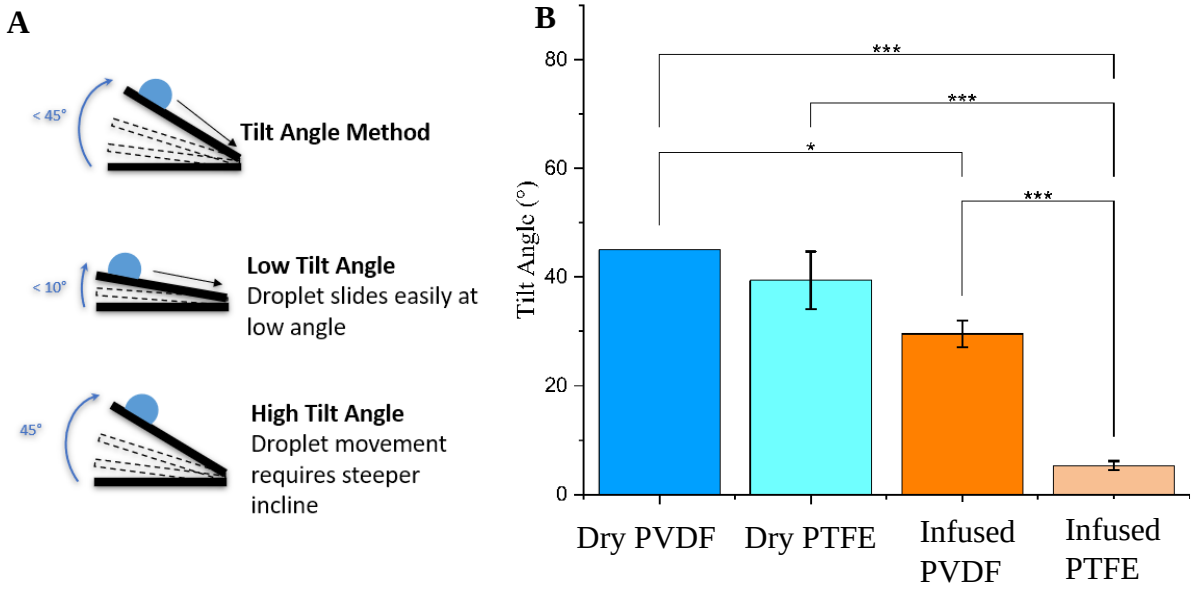

Figure 2: (**A)** Diagram of tilt angle method. **(B)**Tilt angle results for dry PVDF, PVDF infused with K103, dry PTFE, and PTFE infused with K103. A Tukey test was performed to calculate statistical significance. (* p<=0.05, ** p<=0.01, *** p<=0.001)

investigated, Krytox 103 (K103) and Krytox 107 (K107). Both are PFPE, but the viscosities are different, with K103 having a viscosity of 30 cSt at 40°C[36] and K107 having a viscosity of 450 cSt at 40°C[37]. The permeance of K103-liquid infused membranes (K103-LIMs) and K107-liquid infused membranes (K107-LIMs) over 10 continuous filtration cycles are compared in **Figure 3**. Both types of infused membrane show permeance that is significantly different than bare compacted membranes ($p<0.001$). This is as expected because the infusing liquid needs to be pushed aside for the water to be able to flow through the pores. If the infusing liquid was being washed away completely, the permeance would be expected to approach that of the bare membrane

since no additional infusing liquid was added between the 10 consecutive cycles. No significant change in the permeance was observed, which indicates that the infusing liquid is stable within the pores of the membranes under pressure and liquid flow.

The biofilm assay of PVDF and PTFE membranes shows that the addition of an

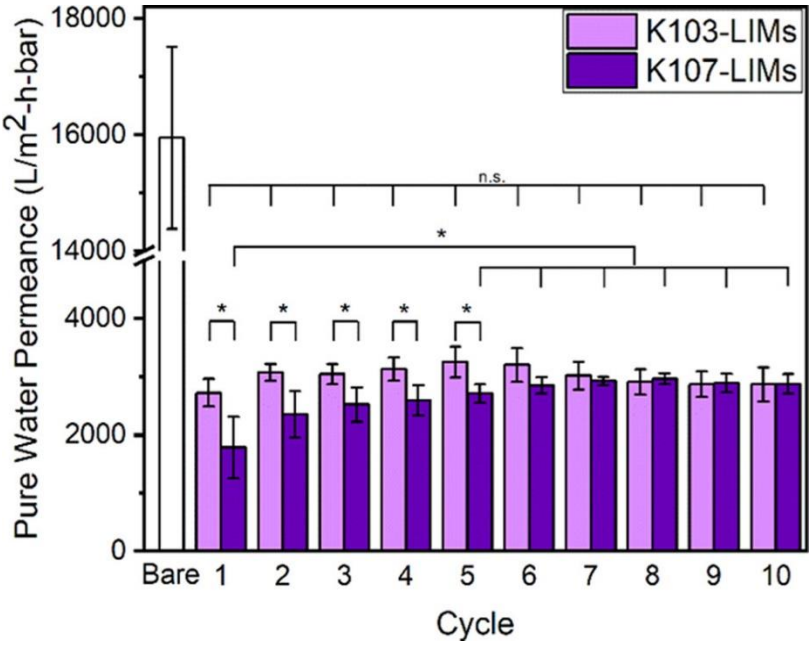

Figure 3: Pure water permeance of liquid infused PVDF membranes from Shah et al[27]. Two different viscosities of perfluoropolyether were investigated as infusing liquids. The initial pure water permeance of compacted bare membranes is provided as a comparison. (*p≤0.05)

immobilized liquid layer reduces biofilm formation for both types of membrane. Shown in **Figure 4A,** infusing PVDF membranes with K103 reduces biofilm formation by approximately 25%, and infusing PTFE with K103 reduces biofilm formation by approximately 98%. Despite not having the same chemical affinity for K103 that PTFE does, the addition of a liquid layer to PVDF improves its anti-fouling properties.

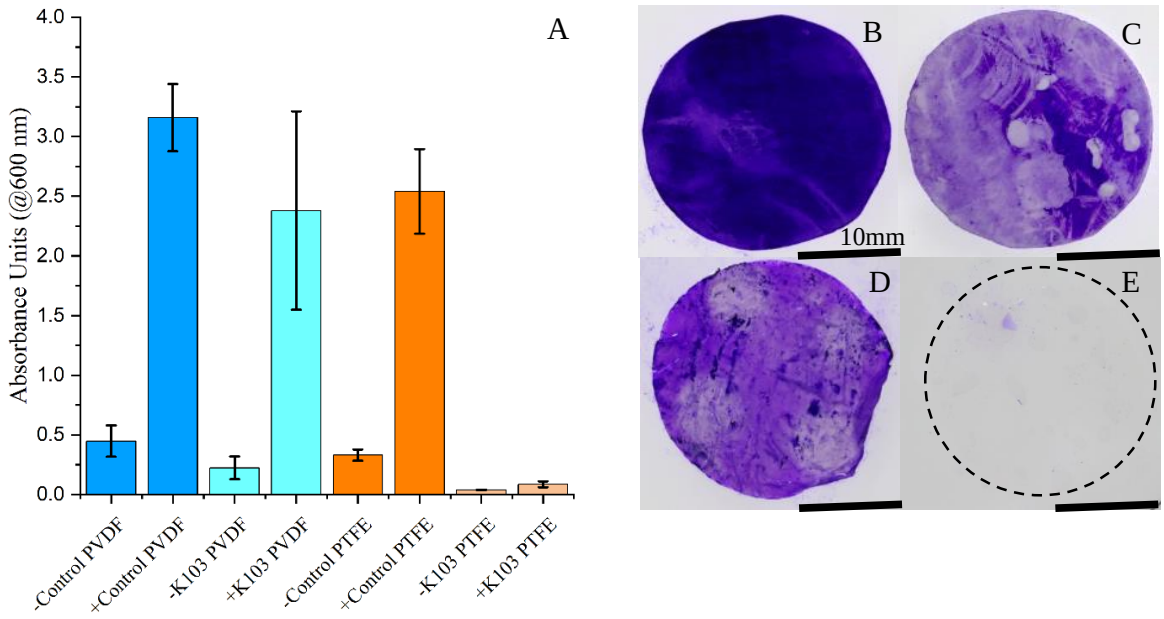

Figure 4: (A) Absorbance measurements (600nm) of the crystal violet extracted with ethanol from biofilm assays of PVDF and PTFE Membranes normalized to the absorbance of pure ethanol. (-) shows that there are no bacteria present in a sample. (+) shows that the media was inoculated with *S. epidermidis* and formed a biofilm. **(B)** Crystal violet-stained biofilm on PVDF control (+ Control PVDF). **(C)** Crystal violet-stained biofilm on PVDF infused with K103 (+K103 PVDF). **(D)** Crystal violet-stained biofilm on PTFE control (+Dry PTFE). The lighter colored circles show where the ceramic weights were used to weigh down the sample in the media. **(E)** Crystal violet-stained sample of PTFE infused with K103 that was grown in conditions that would cause biofilm formation (+K103 PTFE). A dashed circle was added to show the outline of the infused membrane because the addition of K103 to PTFE causes the membrane to become clear.

Conclusion

Based on the biofilm formation assay, the addition of an immiscible-liquid layer to PVDF membranes results in improved resistance to bacterial biofouling despite not performing well in traditional surface characterization tests. The surface characterization tests were showing that the liquid layer was not well formed and was easily displaced by water droplets. Based on these results, the PVDF membranes were expected to not be able to resist bacterial biofilm formation and that the liquid would be washed away easily in water filtration testing. This was not the case, as shown by the results by Shah et al[27]. The infusing liquid was shown to be stable under pressure and over time in water filtration applications. These results, combined with the improved resistance to biofouling shown in by the biofilm assay, show that infused PVDF membranes show promising potential for improving fouling resistance in filtration applications.

CHAPTER 3: PTFE/HEPA MEMBRANES FOR AEROSOL FILTRATION

Note: Portions of the chapter appear in

Regan, D. P., Fong, C., Bond, A., Desjardins, C., Hardcastle, J., Hung, S.-H., Holmes, A. P., Schiffman, J., Maginnis, M., Howell, C. Liquid-infused filters improve the recovery of captured airborne bacteria and viruses (in preparation)

Background

The frequent collection of airborne pathogens for identification can aid in the monitoring of high-risk environments such as hospitals, airports, and other public spaces and can help fill critical knowledge gaps in the study of aerosol transmission routes[38–42]. The development of robust biosurveillance systems will contribute to the tracking of strain mutations and shifts in genomics and proteomics of new pathogens as they spread[38,43].

There are two current methodologies for monitoring airborne pathogens[44,45]. Liquid impingers are used when the viability of the collected sample is the priority, but these systems face challenges such as sample loss, re-aerosolization, and low efficiency[44–46]. Filter based sampling has a higher range for particle size capture, but the samples are often damaged due to desiccation and impaction[45,47]. In order to combine the benefits of both types of systems, modifications need to be made to filter based sampling.

Novel Solid-Liquid Pairings for Immobilized Liquid Layers

The results from the previous chapter show that PVDF filters being used in a water filtration system allow for a PFPE infusing liquid to be stable within the pores under pressure[27]. This demonstrated that despite a lack stability as shown through established surface characterization testing, the presence of the liquid layer on the membrane under pressure can alter the performance the membrane. PVDF does not have the same chemical affinity for the perfluoropolyether that PTFE does due to the reduced number of fluorine atoms. The performance

of the liquid layer under pressure despite the lack of chemical affinity prompted the testing of other types of filtration materials with the infusing liquid that would not normally perform well in surface characterization testing. High efficiency particulate air (HEPA) filters are used to drastically reduce the number of particles, including bacteria and viruses in the air by up to 99.9%[48]. In this study, the HEPA filters used were made from melt blown polypropylene fibers. Polypropylene has zero fluorine atoms, but was explored based on the successes of PVDF membranes that had less fluorine atoms than the PTFE membranes.

Filter Preparation

PTFE membranes with a pore size of 1.0 µm diameter were purchased from Sterlitech. Four groups of infused PTFE membranes were created based on high vs low viscosity of PFPE, and high vs low volume of PFPE. K103 was used as the low viscosity PFPE (82cSt), and K107 was used as the high viscosity PFPE (1535 cSt)[43]. High volume infusion was 160 µL, low volume infused was 80 µL. HEPA samples were cut from H13 HEPA filters (Nanjing Blue Sky Filter Co.) to a diameter of 17 mm. HEPA samples were infused by adding 160 µL K103 dropwise and the excess was allowed to drain.

Surface Characterization

Dry control PTFE and HEPA filters were used to conduct contact angle measurements. A 10 µL droplet of DI water was placed onto each of the dry control filter surfaces. Each filter was tested in three locations. Images were taken with and EOS 5D Mark II camera (Canon) and measured using the low-bond axisymmetric drop shape analysis ImageJ plugin.

Aerosol Filtration

An aerosol filtration system was constructed based on previous studies[43,49], and the flow diagram can be seen in **Figure 5**. Air in-take filter and in-line filters were Vacushields from Fisher Scientific. Diffuser is a Philips Healthcare Innospire Go portable mesh nebulizer. Vacuum pump was a JB industries DV-200N Refrigerant evacuation pump with 7cfm displacement, ½ HP, 115 V, and 7.5 A. Filter samples were tested in the aerosol filtration system by being placed into the filter housing, marked as liquid-gated membrane.

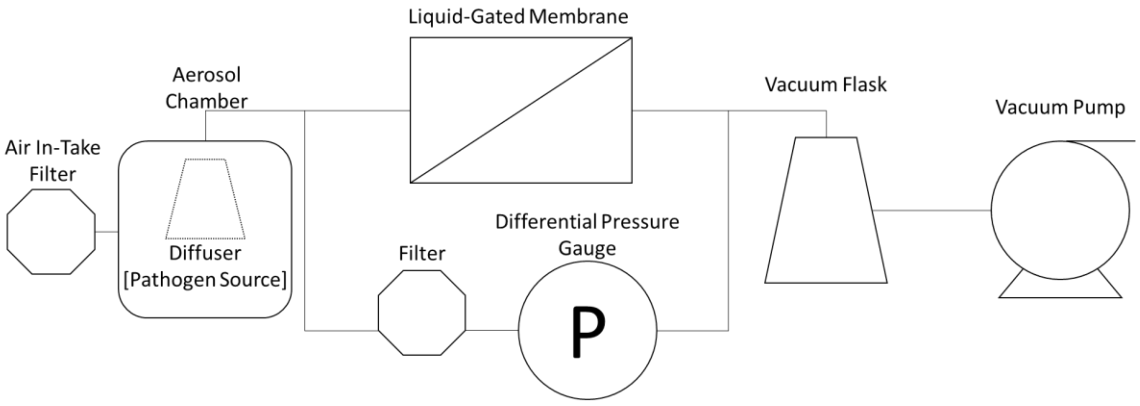

Figure 5: Diagram of aerosol filtration system. Flow moves from left to right

The aerosol filtration and bacterial studies in this chapter were performed by Dr. Daniel P. Regan[43,49]. *E. coli* stock cultures were grown in 2 mL LB broth overnight at 37°C. The bacteria stock solution was diluted in phosphate buffered saline (PBS) to an absorbance of 0.04 at 600 nm. This bacterial dilution was used to fill the diffuser for all filtration runs.

To prime the system for bacterial aerosol testing, the system was run for 15 minutes before testing any filter samples. The diffuser was turned on, the aerosol chamber was closed, and the vacuum pump was turned on. After 15 minutes, the system was primed for use. Each sample was tested by running the vacuum without the diffuser for 1 minute, then running both the diffuser and

the vacuum for 6 minutes, and then another 1 minute with just the vacuum. The sample was then placed in a conical tube to rest for 15 minutes. After resting, the filter was stamped onto a square LB agar plate 9 consecutive times. Each stamp was performed by placing the side of the filter the was upstream in the system down onto the agar surface and then pressing gently with the back of curved forceps. The plates were then incubated at 37°C overnight before conducting CFU counts.

Crystal Violet Assay

A crystal violet assay was performed with 0.01% crystal violet. HEPA samples (dry and liquid-infused) were submerged in the crystal violet solution for 10 minutes, rinsed twice with DI water, allowed to air dry, and then imaged. The images were processed in ImageJ for % coverage based on a threshold value. This was used to estimate how much of the filter was stained with crystal violet compared to how much resisted the stain. In ImageJ, the images are converted to 8-bit and the background is removed. The threshold value is set to 140 on a scale of 0 to 255 (0=black, 255=white), and the fraction area tool is used to measure the fraction of pixels that are below a value of 140 out of the total number of pixels. This value gives the fraction of area that has been stained by crystal violet compared to the total area of the filter.

Results and Discussion

HEPA filters that were uncoated or that had been infused with K103 were unable to be characterized with traditional surface characterization tests because the surface is too porous and rough. The outer shell of the HEPA filter is made of larger fibers that prevent larger debris from reaching the interior of the filter. This prevents the use of established surface characterization testing methods such as contact angle or tilt angle.

The filtration of bacterial aerosols yielded high variability due to many factors. The priming step was added to the protocol to saturate the system with bacteria to mitigate the change seen over time during a run. For this system, there was no way to ensure that the same volume of the bacteria dilution was aerosolized for each sample, or that all of the bacteria that were aerosolized reached the filter samples.

There was no statistical difference seen between sample types for PTFE after the first bacterial removal cycle CFU count, as seen in **Figure 6B.** This suggests that there is no difference in the initial rate of bacterial recovery from the surface of PTFE. PTFE is hydrophobic without PFPE, but becomes ultra-slippery when infused. **Figure 6C** shows that a significant difference in the normalized CFU count is not seen until the third removal cycle for high and low volume infusions of the high viscosity samples ($p \leq 0.006$).

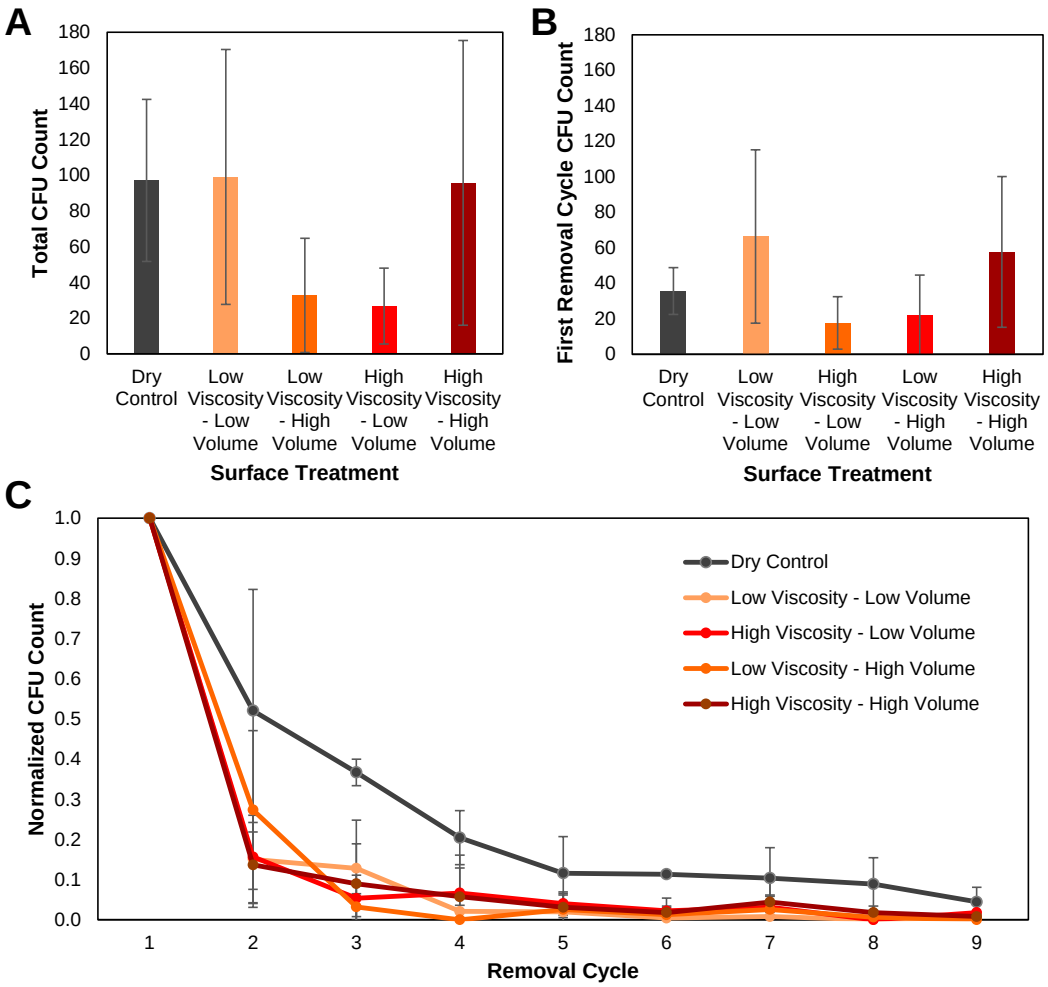

Figure 6: Cumulative colony-forming unit (CFU) count of **(A)** all nine removal cycles and **(B)** CFU counts for the first removal cycle only for dry PTFE controls and varying viscosities and volumes of PFPE. There were no significant differences between the sample groups. **(C)** Normalized release rate for each cycle of bacteria removal. Both the high volume and the low volume – high viscosity samples released bacteria faster than the dry controls, which resulted in a significant difference in normalized CFU counts by the third cycle ($p \leq 0.006$). Figures taken from Regan et al 2022 (in preparation)[43].

Figure 7A shows that infused HEPA samples yield no statistical difference for the first bacteria recovery cycle CFU count, or in total recovery CFU count in **Figure 7B**. Infused HEPA filters displayed a higher and more consistent release rate than dry HEPA controls, shown in **Figure 7C**. The polypropylene fibers in HEPA filters most likely retain PFPE via capillary forces, which form a liquid net that stabilizes the capture and release efficiency for liquid net filtration.

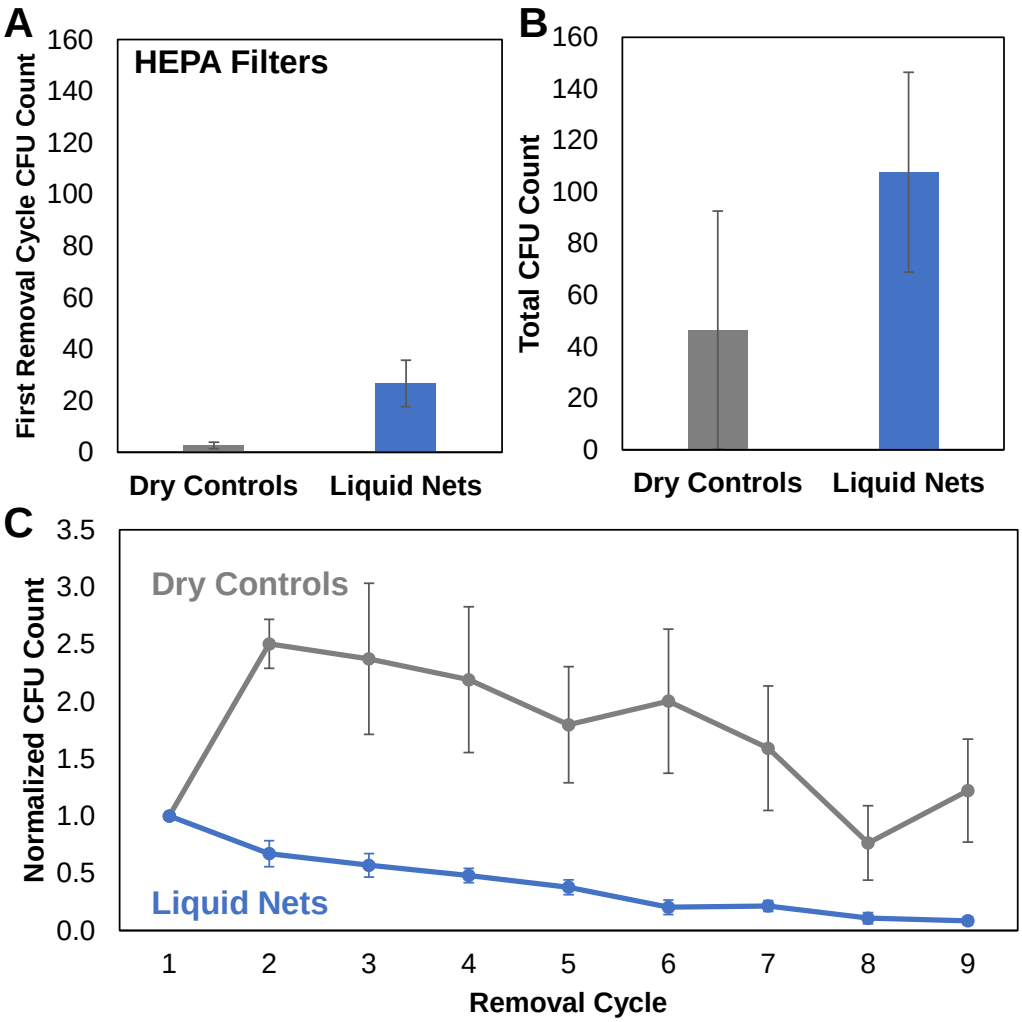

Figure 7: (A) CFU counts of first removal cycle **(B)** and total CFU counts for dry HEPA control filters vs HEPA filters infused with PFPE. There were no significant differences between sample groups. **(C)** Normalized release rate for all nine bacteria removal cycles. Figure taken from Regan et al 2022 (in preparation)[43].

To characterize the effectiveness of the added liquid layer, the crystal violet assay was used. In **Figure 8A,** the results of the crystal violet assay have been quantified via ImageJ analysis. The 140-threshold level was chosen based on visual estimation. The threshold level was adjusted until it was able to distinguish between visually stained portions of the filter and unstained portions. The HEPA control that was not infused can be seen in **Figure 8B(i)**, and the HEPA filter that was infused with K103 can be seen in **Figure 8B(ii)**. The amount of staining from the crystal violet between the two sample types is significant ($p \leq 0.001$). The infused HEPA filter resisted crystal violet staining despite not having any chemical affinity for the infusing liquid. This shows that the fluorine pairing from the previous chapter was not the only characteristic for identifying a successful match of infusing liquid and solid substrate.

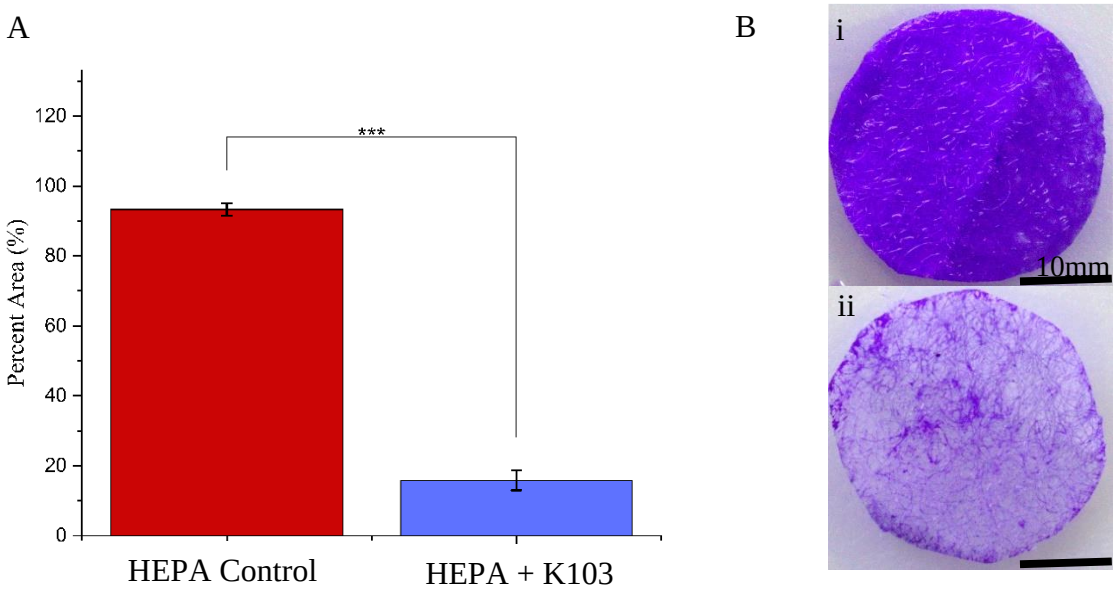

Figure 8: (A) % coverage analysis of HEPA filter after crystal violet assay. Statistical significance was calculated with a Tukey Test. (***$p \leq 0.001$) **(B)** Dry HEPA control after crystal violet staining **(i)** and HEPA filter infused with 160µL K103 after crystal violet staining **(ii)**

A potential biosurveillance device is outlined in **Figure 9**. A bioaerosol source releases particles containing bacteria or viruses, which are then captured by an air purifier. The modification that could improve sample viability and aerosol capture efficiency is within the membrane itself. A dry membrane currently requires mechanical or chemical collection techniques that may reduce sample viability. A membrane with a liquid net could be added to an air purifier to improve collected sample viability and allow for greater sample collection. Above the critical pressure, the pores of the liquid net would open, allowing for air flow through the filter. When the pressure is reduced below the critical pressure, the liquid layer reforms, pushing the captured pathogens out of the pores and to the immobilized liquid layer surface. This phenomenon would allow for the improved capture efficiency of a filter-based sampling system, and the improved viability of a liquid-based capture system to be combined into one.

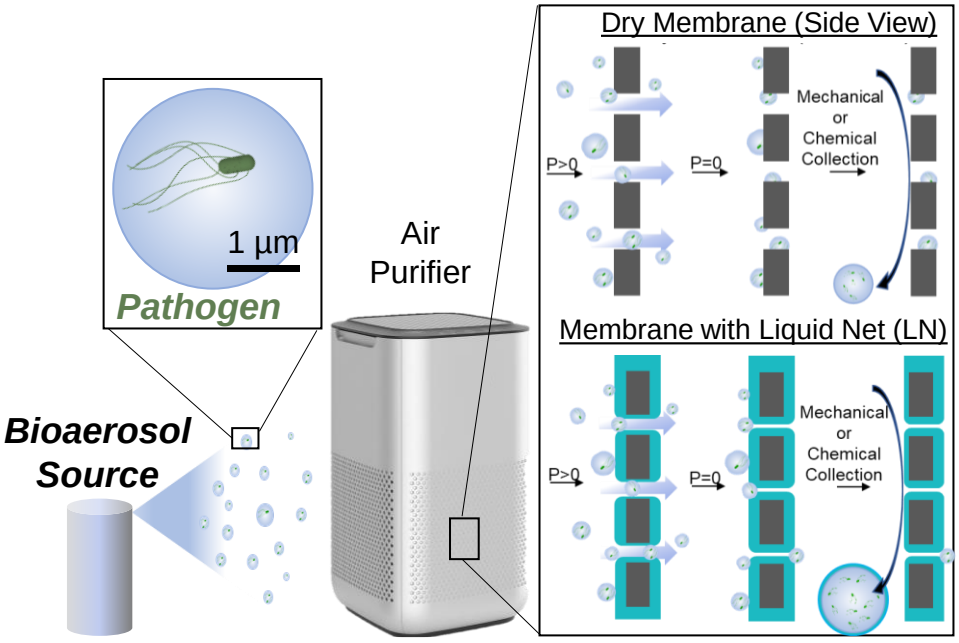

Figure 9: Schematic description of the experimental concept. Figure from Regan et al 2022 (in preparation)[49].

Conclusion

Infused HEPA filters show improvements in rate of release and yield a more consistent release than dry controls, show no difference in total bacterial recovery. A difference in the first recovery cycle may be seen, but additional testing is required to show significance. HEPA filters infused with PFPE were able to successfully resist crystal violet staining. This is a promising result that shows that chemical affinity and surface characterization testing are not the only defining factors for identifying potential solid-liquid pairings for creating immobilized liquid layers. The success of infused PVDF in the previous chapter and the success of infused HEPA filters open up the path forward for testing new pairings. Filter characteristics such as surface morphology, porosity, pore geometry, and more are likely reasons that these materials are able to support a liquid layer despite not having optimum chemistry for doing so. The liquid layer may be supported via capillary action and surface tension instead of through primarily chemical affinity. Further testing is required to identify the limits of infused HEPA filters and its stability under extended use. The addition of a PFPE liquid layer decreases efficiency and increases the pressure drop in the system, but shows improvements to bacterial recovery and fouling resistance. This trade off will need to be considered when applying this concept to larger systems and in other applications.

CHAPTER 4: SUSTAINABLE HYDROPHOBIC PDMS COATED PAPER FILTERS

Background

Many filtration materials and immobilized liquid surfaces rely on the use of per- and poly-fluoroalkyl substances (PFAS). PFAS are defined by the presence of the perfluoroalkyl moiety C_nF_{2n+1}-. Perfluoroalkyl moieties are highly chemically and thermally stable and are both hydrophobic and lipophobic[50]. These properties make PFAS highly desirable for use in surfactants and polymers. Polymer applications can include textile stain and soil repellants, food-contact paper, filtration materials, and non-stick coatings[50–52].

There is a growing concern about the use of these forever chemicals in many different industries. The high stability of these chemicals and their widespread use have led to considerable soil and groundwater contamination[53]. PFAS have high environmental persistence with high bioaccumulation potential and associated toxicities[50,53,54]. A major concern for public health is with the major risk pathway for the bioaccumulation of PFAS through the food chain via drinking water, meat, fish, and milk, and also through food that has been packaged in PFAS-containing materials and indoor dust inhalation[51,53,55]. PFAS are known as endocrine disruptors because they reportedly alter androgen and estrogen-receptor functions[53,56–58]. With the high risk for bioaccumulation, PFAS have been reported in the blood serum and breast milk in humans all around the world[55–57]. Exposure to specific types of PFAS has been shown to affect human health through altered kidney and thyroid function, immunosuppression, and deleterious effects on reproduction and development[56–58]. Perfluoropolyether falls under the PFAS characterization[51,52].

The chemical vapor deposition of polydimethylsiloxane (PDMS) onto various substrates has been shown to create superhydrophobic surfaces that resist corrosion and improve oil/water separation[59,60]. On aluminum, contact angles of up to 158.7° have been reported[60]. PDMS has been

used to support immobilized liquid layers by being infused with silicone oil[25,30]. Whatman paper filters are made from cellulose and are a commonly used material in chemistry labs for the separation of solids and liquids and come in a variety of pore sizes for different applications[61]. Chemical vapor deposition of PDMS onto cellulose-based paper filters is investigated for producing a hydrophobic surface and supporting a liquid layer of silicone oil.

PDMS Coated Paper Filter Development

PDMS coated paper filters were produced by adding PDMS base (Sylgaard 184) to fully cover the bottom of a 250 mL Pyrex beaker. Whatman Grade 1 Quantitative Filter Paper was used to cover the top of the beaker and then held in place by tightly covering with aluminum foil. The prepared beaker was then heated slowly with a hot plate inside of a fume hood to 300°C. Once the vapors fully saturated the inside of the beaker and condensation could be seen on the sides, the temperature was held constant for 10 minutes. The hot plate was then turned off and the beaker was allowed to cool to the touch. The PDMS coated paper was then removed and tested for a contact angle. Contact angle was measured by placing a 10µL droplet of DI water at 3 different locations on the treated surface. The droplets were photographed from the side with a Canon EOS 6D Mark II camera with a 100 mm macro lens (Canon, Huntington, NY). The photos of the droplets were analyzed with the Contact angle Plugin for ImageJ[62].

To increase production of PDMS coated paper filters, a new system was created for suspending the filters in the PDMS vapors. Paper filters were cut from Whatman Grade 1 Quantitative Filter Paper to a diameter of 19mm and placed onto racks made of steel mesh and were suspended at two different heights within a 1L Pyrex beaker by aluminum wire, shown in **Figure 10**. Enough PDMS base was added to completely cover the bottom of the beaker and the

racks were suspended at 5cm and 9cm above the surface of the PDMS base. The beaker was then covered tightly with aluminum foil and heated slowly to 300°C. The beaker was held at saturation for 10 minutes and then allowed to cool to the touch. The filters were then removed from each layer carefully to ensure the top and bottom were oriented correctly for testing. Contact angles were measured for the top and bottom of each filter on each height layer. The weight change of each filter from PDMS coating was tracked. Each filter was weighed before treatment and after, and the position of each filter was tracked throughout the entire process so that the weight change could be correctly calculated.

The next stage of the process development was increasing the time held at saturation to 30 minutes in effort to increase the coating efficiency. To reduce the amount of variability between filters for contact angle and weight change from coating, and to increase the number of filters that

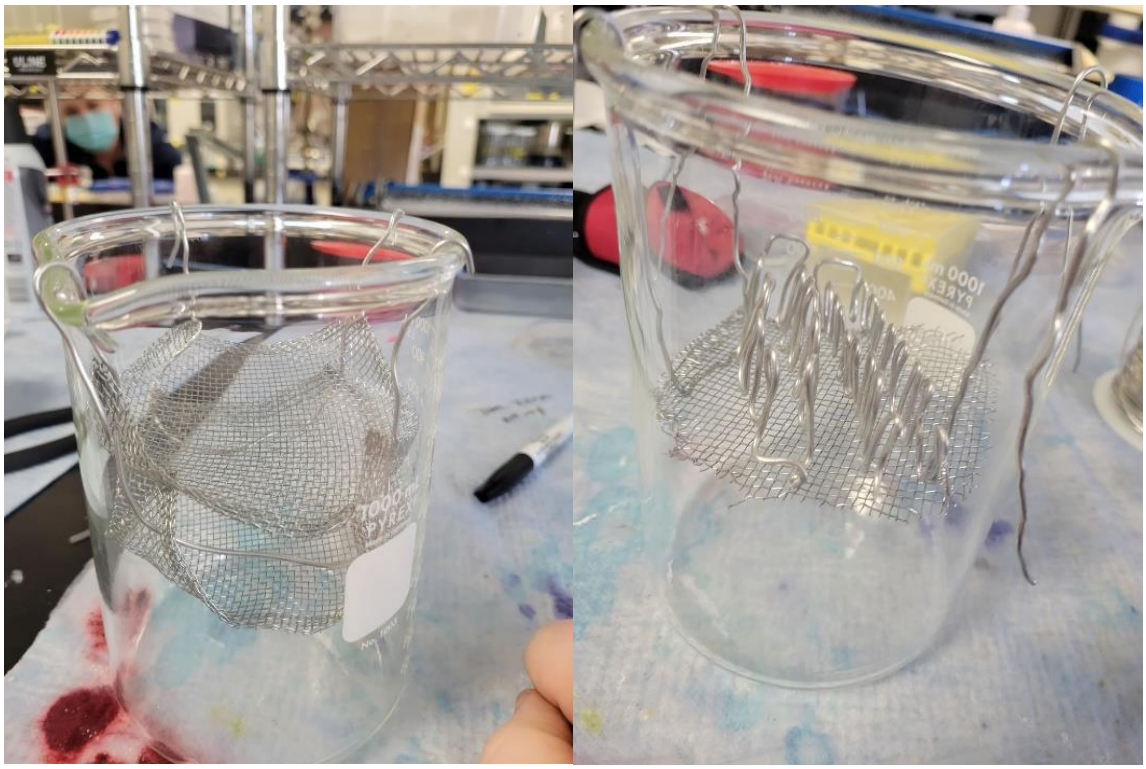

Figure 10: (left) Bilayer horizontal setup for chemical vapor deposition of PDMS. Layers are 5cm and 9cm above liquid surface. (right) Vertical setup for chemical vapor deposition of PDMS. Layer is 5cm above liquid surface and can hold 20 samples at a time for coating.

could be coated per batch, a rack was constructed from aluminum wire that would hold the filters vertically on top of a steel mesh rack at the 5 cm height layer, as shown in **Figure 10**. This vertical orientation allowed for 20 PDMS coated filters to be produced per batch. Filters at this stage were tested for contact angle and weight change.

To prepare samples for Scanning Electron Microscopy (SEM) imaging, a baking step was added to ensure that samples were dry. Samples were baked overnight at 70°C in an Isotemp Oven. SEM imaging was performed on uncoated filters and PDMS coated paper filters that had been baked. This baking step was included for all PDMS coated samples after this point. Samples were sputter coated with a 6nm layer of gold-palladium. SEM imaging was performed using an AMRay 1820 with 5 kV accelerating voltage and magnifications of 1 kX and 2.5 kX. Image capture was performed with and iXRF digital-capture system.

To produce infused samples, two infusion methods were tested. The first method was adding 150 µL of silicone oil (10cSt polydimethylsiloxane, trimethylsiloxy terminated) per filter (approximately 53 $\mu L/cm^2$) and then draining vertically for 10 minutes. The second method was fully submerging the samples in silicone oil for 30 minutes and then draining vertically for 10 minutes (long soak method). These infused samples were then tested for weight change after infusion to calculate silicone oil uptake.

To test if samples were viable for use in air filtration, samples were tested in the aerosol filtration system described in Chapter 3, Aerosol Filtration, and the transmembrane pressures were measured during a 5-minute filtration cycle. To test if the pores were still open after coating and infusion, a liquid filtration system was created. Samples were placed in a 2 mL Buchner funnel that was attached to a vacuum flask with a small electric pump. Using a serological pipette, 10 mL of DI water was added to the Buchner funnel with the electric pump running, and the time to filter

the entire volume was measured. For both aerosol and liquid filtration, untreated control paper filters, PDMS coated paper filters, and infused PDMS coated paper filters (both methods) were tested.

The ability for the PDMS coated paper filters to resist the adhesion of contaminants was evaluated with a crystal violet assay. Samples were dipped in 0.01% crystal violet for 5s, washed in DI water twice, and then allowed to dry. These samples were imaged and then the crystal violet was extracted with 1.5 mL ethanol for each sample. The CV extract was then analyzed with a spectrophotometer by measuring the absorbance at 600 nm after being normalized to pure ethanol.

Results and Discussion

Early treatment methods for producing PDMS coated paper filters showed a lot of variability and were not always successful. Shown in **Figure 11**, the variability within the two-layer horizontal setup can be seen. There are differences between the tops and the bottoms of the filters, and between heights. Each group in these often had some samples that were considered failed treatments because the water droplet would soak into the filter during the contact angle test. This showed that the coating treatment was inconsistent and not always effective. This could be also seen because some filters would come out of the treatment with some spots that appeared wet. These spots are most likely explained by two potential causes. First is that the PDMS was boiling too aggressively and would sometimes pop or splash so that a drop of it would hit some of the filters. This is possible for the 5 cm height layer, but not the 9 cm layer because the drop would have to go through two steel mesh screens and a layer of samples to do so. Second, is that the steel mesh was causing the vapors to condense back into a liquid form which would then soak into the paper filters at certain contact points. This could also help explain some of the variability between the top and bottom layers of the filters.

To further optimize the production method, the vertical orientation set up was created. This allowed for all of the samples in a batch to be produced at the same height (5 cm above liquid) and for a total number of samples produced at a time to increase to 20 filters. The number of contact points with any metal was also reduced to limit the effects of any condensed liquid on the metal surfaces. The vertical orientation allowed for a more uniform flow of the vapors across the surface of the filters on both sides. This addressed the issue of variance between sides of the filters that the horizontal orientation produced. The 30-minute time at vapor saturation was retained after the

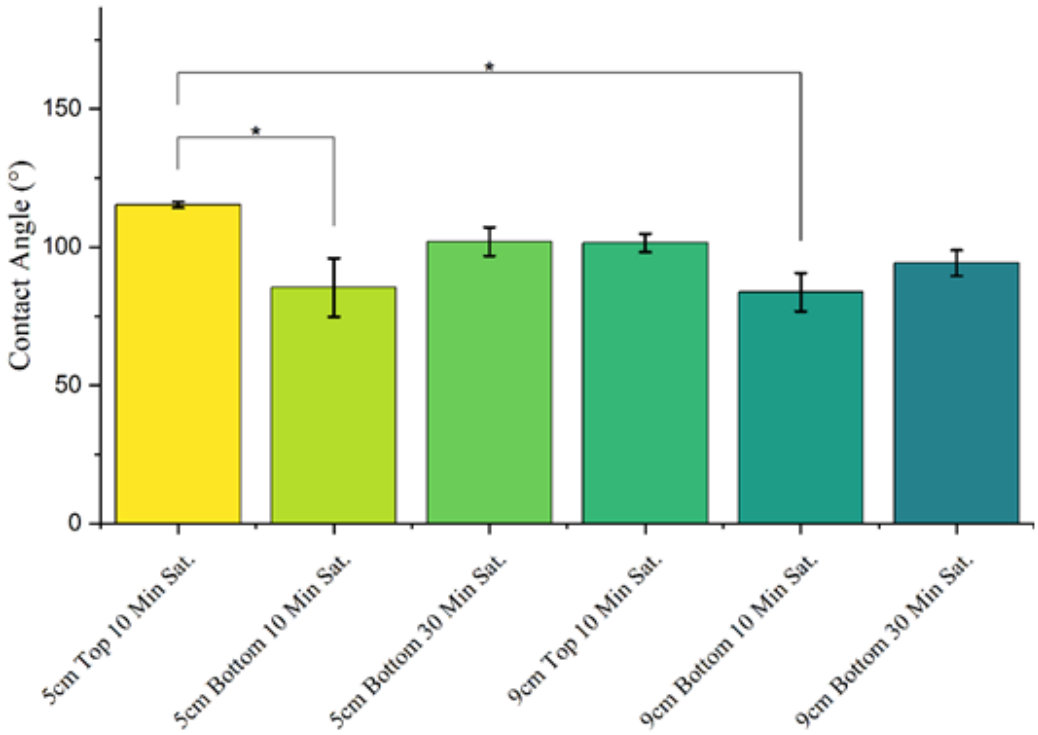

Figure 11: Contact angle results for PDMS coated paper filters at different heights in the two-layer setup, top and bottoms of filters, and different times held at saturation. A Tukey test was used to test for significance. (* p<= 0.05)

vertical setup was implemented because the number of failures (water soaking into filters during

contact angle testing) was reduced to zero. The vertical orientation with 30 minutes at saturation yielded an average contact angle of 96.5±11.4°.

Baked samples of PDMS coated paper filters and dry samples were imaged using SEM imaging. **Figure 12A** shows a baked PDMS coated paper filter at 1000X and it can be seen that some of the finer details and strands of cellulose fibers are missing that can be seen in the dry control in **Figure 12C**. This means there is either these smaller fibers are missing in the PDMS coated samples or that there is an additional layer that is coating the fibers to make them appear larger or forcing them to adhere to larger fibers. This can be seen more clearly at 2500X in **Figure 12B**, where absolutely no fine fibers can be seen. During the imaging steps, the intensity of the electron beam seemed to be melting the PDMS, which is why the surfaces appears smoother and more liquid-like. The appearance of this PDMS coated surface is drastically different than the surface of the dry control at 2500X seen in **Figure 12D.**

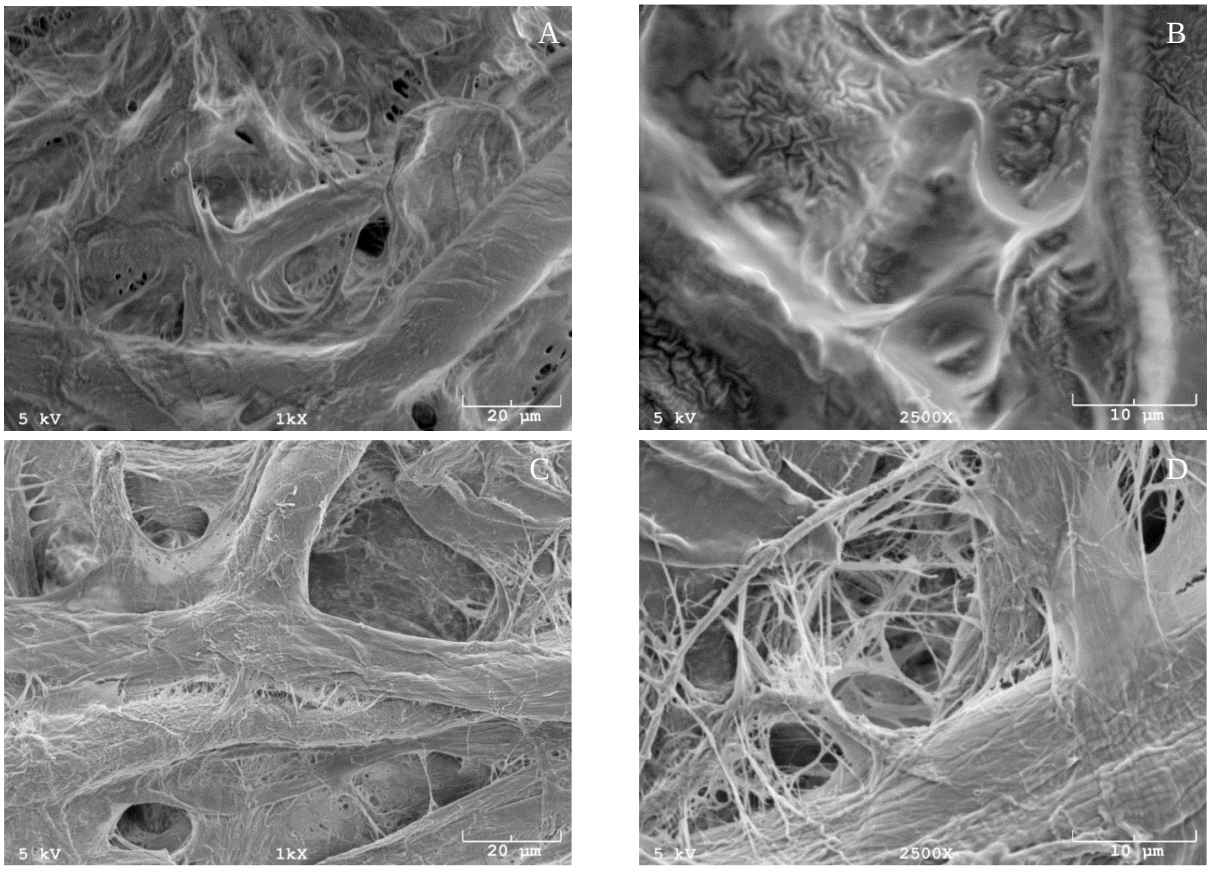

Figure 12: SEM images of **(A)** Baked PDMS coated paper at 1000X, **(B)** Baked PDMS coated paper at 2500X, **(C)** Uncoated dry paper filter at 1000X, and **(D)** Uncoated dry paper filter at 2500X

To characterize how much silicone oil was supported in a liquid layer by these baked PDMS coated filters, the weight before and after infusion with silicone oil by two different immersion methods was tracked. The first method was by adding silicone oil drop wise and then draining the excess. The second method was by immersing the samples completely in silicone oil for 30 minutes and then draining for 10 minutes. The weight change from each of these methods can be seen in **Figure 13.** The weight of the infused silicone oil was calculated by subtracting the pre-infusion weight from the post-infusion weight. This gives the amount of silicone oil that was absorbed by each membrane. There is a significant difference between the baked PDMS samples that underwent a long soak infusion and either control method as seen in **Figure 13**. This shows

that this layer soaked up less Si oil than the control. This can be explained by two sets of reasoning. Either the PDMS coated the filter so that the Si oil could not soak into the cellulose fibers as efficiently, or it had already caused the cellulose fibers to swell so there was less room for the Si oil to cause swelling. This was a different result than expected because the PDMS was expected to swell to support an immobilized liquid layer of the Si oil.

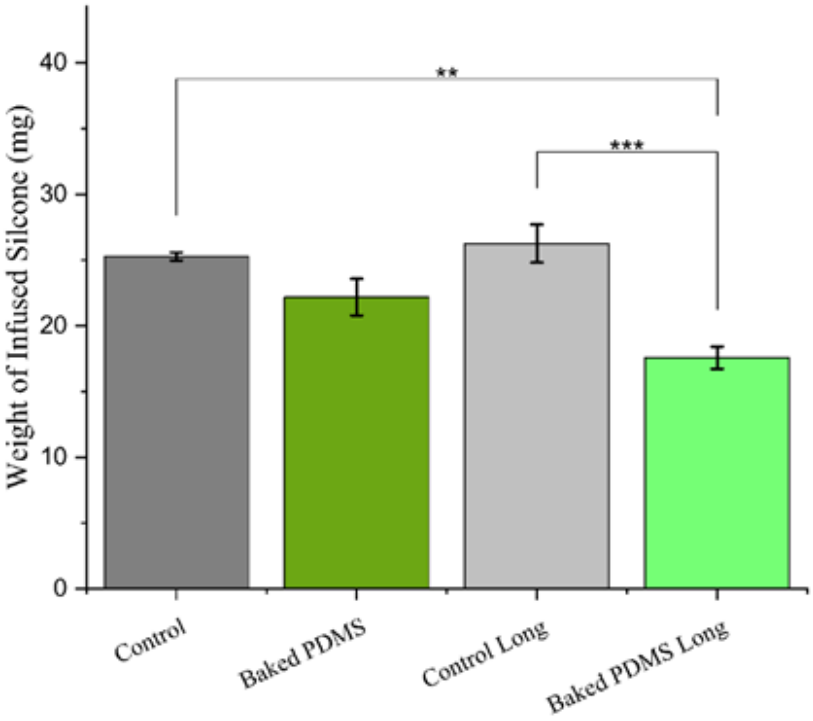

Figure 13: Weight change from silicone oil infusion by two methods of infusion. Control samples were uncoated paper filters. First method was adding Si oil dropwise and draining, and second method was the long soak method. A Tukey test was used to test for significance. (* p<=0.05, ** p<=0.01, *** p<=0.001)

Filtration Efficiency

The transmembrane pressures of samples with and without silicone oil were measured and can be seen in **Figure 14A.** There is no statistical difference seen between any sample type. This suggests that the addition of a PDMS coating or a silicone oil layer does not reduce filter efficiency in terms of flux. The time to filter 10mL of DI water in a vacuum flask was timed for each sample type and can be seen in **Figure 14B.** The only sample type that took significantly longer to filter was the uncoated paper filter with Si oil. This means that the presence of silicone oil without a PDMS coating reduces the flux of DI water in a water filtration application. After 3 cycles of filtration, the PDMS coated samples were still able to prevent a drop of water soaking in after being removed from the vacuum filtration system. This suggests that the PDMS coating is stable and not able to be easily washed away by water.

The crystal violet assay of the samples demonstrated that the PDMS coated samples are able to more easily resist staining than untreated samples. As seen in **Figure 15,** samples that had not been treated with PDMS, with or without silicone oil, were stained much more fully with crystal violet. This shows that the PDMS coating of the paper filters not only causes the paper filters to be more hydrophobic, but also that they are able to prevent the adhesion of an aggressive stain.

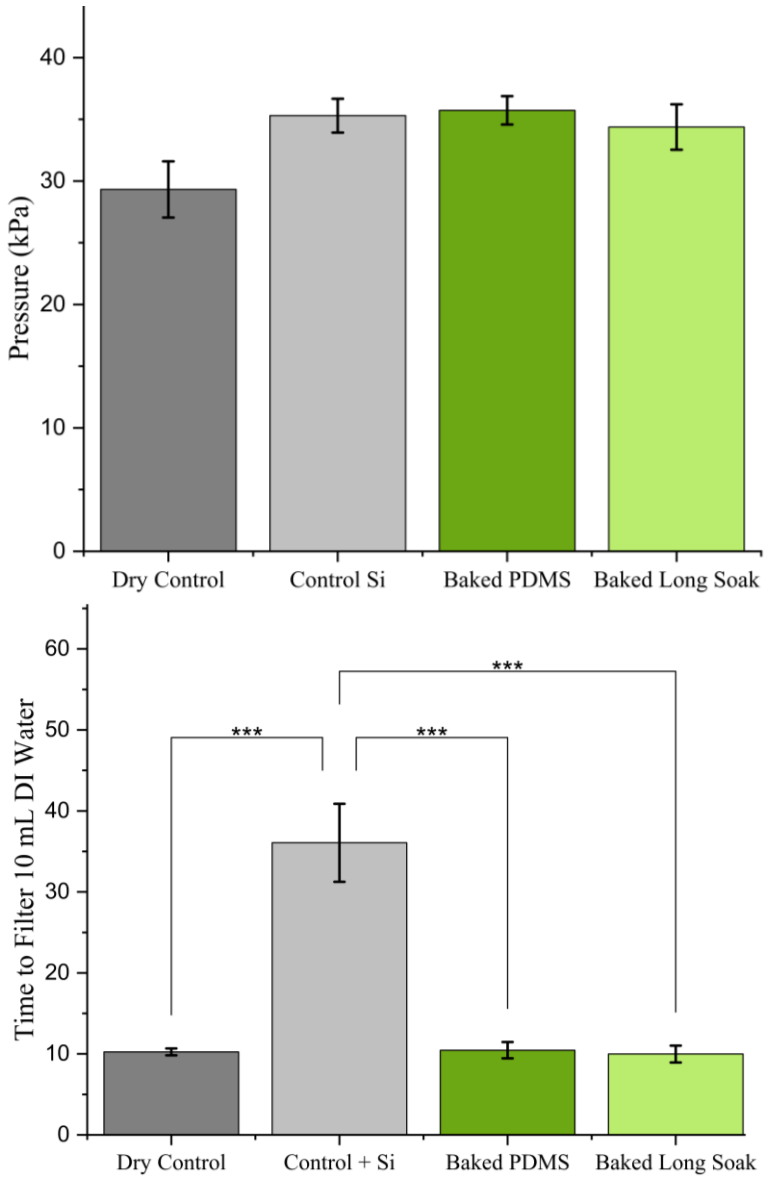

Figure 14: (A) Transmembrane pressures of samples in the aerosol filtration system. No statistical significance was seen between any sample type according to a Tukey test. **(B)** The time to filter 10 mL of DI water in a vacuum flask. The only sample type that was significantly different is the uncoated control with Si oil.

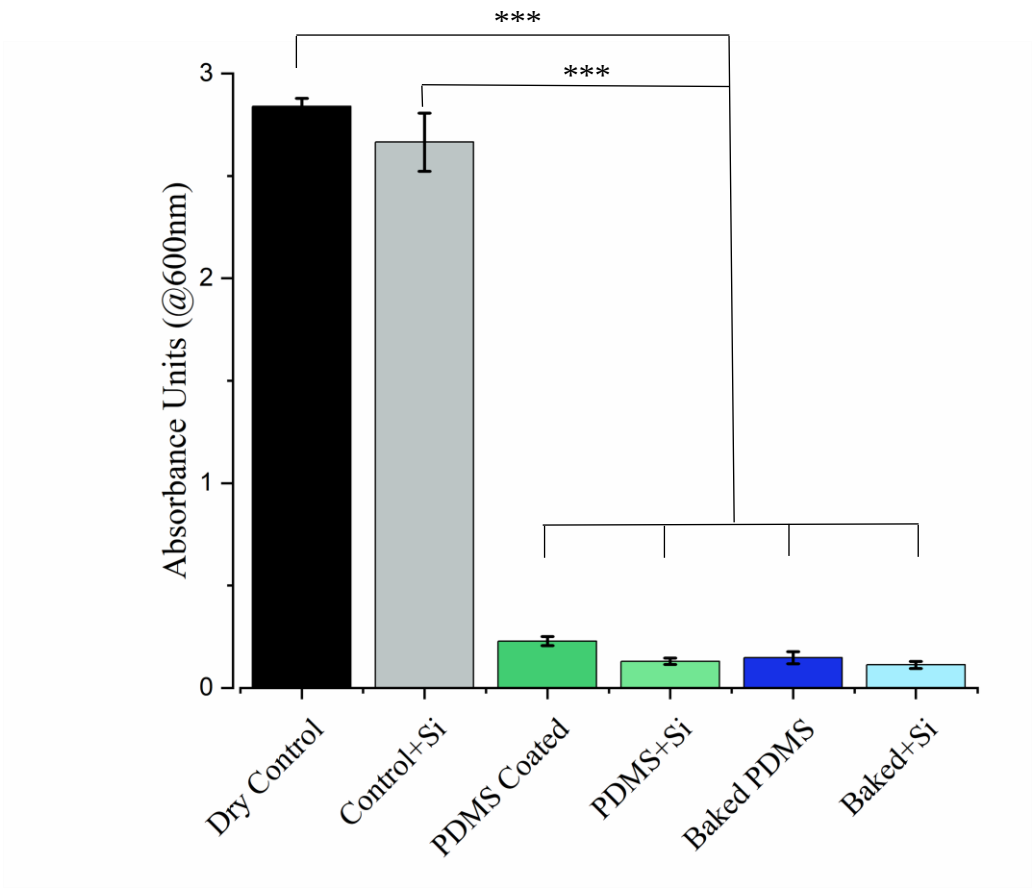

Figure 15: Absorbance at 600nm of the CV extract of samples after a crystal violet assay. Values have been normalized to the absorbance of pure ethanol at 600nm. Statistical significance was done with a Tukey Test. (***$p \leq 0.001$)

Conclusion

PDMS coated paper filters still require optimization to be applied to more robust filtration applications. The results in this chapter demonstrate a successful treatment method that allows for a hydrophobic material to be created from an inexpensive hydrophilic substrate. This treatment does not block the pores in water nor air filtration. The PDMS coating adds a layer of protection that resists crystal violet staining and indicates that fouling can be reduced. The stability of the Si oil layer still needs to be investigated, and may require the testing of a variety of viscosities in order to create an optimized version.

CHAPTER 5: CONCLUSIONS AND FUTURE WORK

Membrane fouling leads to the accumulation of a variety of costs in filtration systems. Fouling leads to a decrease in filtration efficiency, an increase in the frequency of chemical and mechanical cleaning techniques, and a decrease in membrane lifetime. The combination of these factors increases system cost and process downtime. Addressing these problems requires novel solutions in terms of filtration materials. Preventing the adhesion of contaminants such as bacteria, can reduce the initial step of biofilm formation, bioadhesion. Anti-fouling properties have been observed with the use of SLIPS, and these ideas have been applied to filtration materials for multiphase separation processes.

Infused PVDF membranes can be used to support an immobilized liquid layer of a perfluoropolyether infusing liquid, despite not having an optimized chemical affinity for it. PVDF membranes were able to show notable improvements by being infused in functional testing even though surface characterization tests predicted poor performance. According to the surface characterization tests, the liquid layer was not well worked and could easily be displaced. This was disproved based on functional tests such as the biofilm formation assay and the results of the pure water permeance tests of Shah et al[27]. These successful results paved the way for future work with different solid-liquid pairings to identify new materials for the creating of solid-liquid layers.

Infusing HEPA filters with PFPE yields a trade-off. The addition of a liquid layer on HEPA filters allows for the resistance of crystal violet staining, which suggests that other contaminants, such as bacteria, would also display reduced adhesion. The presence of the liquid layer also decreases efficiency and pressure drop across the membrane. Infused HEPA shows improved bacterial recovery with the first cycle, but no difference in total recovery. Overall, the rate of bacterial recovery is more consistent than dry controls. This solid-liquid pairing will require further

optimization to begin approaching use in a biosurveillance system for public health monitoring. Further work to characterize sample viability after recovery would need to be done before being compared to current methods for air sampling.

Future work with PVDF will be to characterize the functional performance over time with liquids containing bacteria and foulants instead of pure water. These future studies will also need to investigate different cleaning techniques for these infused PVDF membranes. The cleaning techniques developed will need to allow for the liquid layer to be retained during cleaning or will need to include a replenishing step before restarting filtration. The goals of these new methods will to be reduce the frequency of cleaning, time and resource costs of cleaning, retaining filter efficiency, and extending the lifetime of a filter.

Sustainable PDMS coated paper membranes are still in the early stages and there is a lot of work that needs to be done before they can be useful. The success of this work has been to create a hydrophobic filtration material from an inexpensive and sustainable hydrophilic material. The stability of the silicone oil layer has not been investigated nor fully optimized. Future work will include a collaboration with the University of Massachusetts Amherst to characterize bacterial interactions with the immobilized liquid layer based on a live/dead microscopy study. Other types of paper filters will also need to be tested. Currently, samples have only been created from Whatman Grade 1 paper filters, which have an estimated pore size of approximately 11µm, which would allow for many bacteria to flow through during filtration. Smaller pore sizes will need to be used for bacterial filtration. The only viscosity of silicone oil tested with these filters is 10 cSt, so several other viscosities will need to be tested to identify which will be optimum for different pore sizes. Future work will be testing how bacterial filtration in liquid and aerosol filtrations. Bacteria will be aerosolized and tested in the aerosol filtration system shown in **Figure 5**.

The successes discussed in this thesis will drive the field forward for creating immiscible liquid-coated materials for water and aerosol filtration. The creation of PDMS coated paper filters opens an entirely new category of SLIPS and will likely inspire the treatment of other materials with coatings of PDMS.

REFERENCES

1. Zhang, C., Wang, J., Olah, A. & Baer, E. Composite nanofibrous microfiltration water filter. *Journal of Applied Polymer Science* **134**, 45557 (2017).

2. Rickert, B., Schmoll, O., Rinehold, A. & Barrenberg, E. Water safety plan: a field guide to improving drinking-water safety in small communities. 100 (2014).

3. Disease Threats and Global WASH Killers: Cholera, Typhoid, and Other Waterborne Infections | Global Water, Sanitation and Hygiene | Healthy Water | CDC. https://www.cdc.gov/healthywater/global/WASH.html?CDC_AA_refVal=https%3A%2F%2Fwww.cdc.gov%2Fhealthywater%2Fglobal%2Fdiarrhea-burden.html.

4. Mao, N. Nonwoven fabric filters. *Advances in Technical Nonwovens* 273–310 (2016) doi:10.1016/B978-0-08-100575-0.00010-3.

5. J, J. S. Applications of Ultrafiltration, Reverse Osmosis, Nanofiltration, and Microfiltration in Dairy and Food Industry. *Extensive Reviews* **1**, 39–48 (2021).

6. Ersahin, M. E. *et al.* A review on dynamic membrane filtration: Materials, applications and future perspectives. *Bioresource Technology* **122**, 196–206 (2012).

7. Díez, B. & Rosal, R. A critical review of membrane modification techniques for fouling and biofouling control in pressure-driven membrane processes. *Nanotechnology for Environmental Engineering* **5**, (2020).

8. Pichardo-Romero, D., Garcia-Arce, Z. P., Zavala-Ramírez, A. & Castro-Muñoz, R. Current Advances in Biofouling Mitigation in Membranes for Water Treatment: An Overview. *Processes 2020, Vol. 8, Page 182* **8**, 182 (2020).

9. Bardone, E. *et al.* Description of the Biofouling Phenomena Affecting Membranes by the Boundary Flux Concept. *CHEMICAL ENGINEERING TRANSACTIONS* **49**, (2016).

10. Metzger, U., Le-Clech, P., Stuetz, R. M., Frimmel, F. H. & Chen, V. Characterisation of polymeric fouling in membrane bioreactors and the effect of different filtration modes. *Journal of Membrane Science* **301**, 180–189 (2007).

11. Ang, W. S., Tiraferri, A., Chen, K. L. & Elimelech, M. Fouling and cleaning of RO membranes fouled by mixtures of organic foulants simulating wastewater effluent. *Journal of Membrane Science* **376**, 196–206 (2011).

12. Lin, J. C. te, Lee, D. J. & Huang, C. Membrane Fouling Mitigation: Membrane Cleaning. *https://doi-org.wv-o-ursus-proxy02.ursus.maine.edu/10.1080/01496391003666940* **45**, 858–872 (2010).

13. Hong, S. & Elimelech, M. Chemical and physical aspects of natural organic matter (NOM) fouling of nanofiltration membranes. *Journal of Membrane Science* **132**, 159–181 (1997).

14. Surfactants and Interfacial Phenomena - Milton J. Rosen, Joy T. Kunjappu - Google Books. https://books.google.com/books?hl=en&lr=&id=pdTsgREZp5QC&oi=fnd&pg=PR15&ots=-86EWguUpK&sig=INE_0OeF0QSAh9Oxi5OWKSirnVA#v=onepage&q&f=false.

15. al Aani, S., Mustafa, T. N. & Hilal, N. Ultrafiltration membranes for wastewater and water process engineering: A comprehensive statistical review over the past decade. *Journal of Water Process Engineering* **35**, 101241 (2020).

16. Wu, Y. *et al.* Recent advances in mitigating membrane biofouling using carbon-based materials. *Journal of Hazardous Materials* **382**, 120976 (2020).

17. Flemming, H. C. Biofouling in water systems – cases, causes and countermeasures. *Applied Microbiology and Biotechnology 2003 59:6* **59**, 629–640 (2002).

18. Binahmed, S., Hasane, A., Wang, Z., Mansurov, A. & Romero-Vargas Castrillón, S. Bacterial Adhesion to Ultrafiltration Membranes: Role of Hydrophilicity, Natural Organic Matter, and Cell-Surface Macromolecules. *Environmental Science and Technology* **52**, 162–172 (2018).

19. Mansouri, J., Harrisson, S. & Chen, V. Strategies for controlling biofouling in membrane filtration systems: challenges and opportunities. *Journal of Materials Chemistry* **20**, 4567–4586 (2010).

20. Nosonovsky, M. & Bhushan, B. Biomimetic superhydrophobic surfaces: Multiscale approach. *Nano Letters* **7**, 2633–2637 (2007).

21. Hoek, E. M. V., Bhattacharjee, S. & Elimelech, M. Effect of membrane surface roughness on colloid-membrane DLVO interactions. *Langmuir* **19**, 4836–4847 (2003).

22. Bohn, H. F. & Federle, W. From the Cover: Insect aquaplaning: Nepenthes pitcher plants capture prey with the peristome, a fully wettable water-lubricated anisotropic surface. *Proc Natl Acad Sci U S A* **101**, 14138 (2004).

23. Hou, X., Hu, Y., Grinthal, A., Khan, M. & Aizenberg, J. Liquid-based gating mechanism with tunable multiphase selectivity and antifouling behaviour. *Nature* **519**, (2015).

24. Epstein, A. K., Wong, T. S., Belisle, R. A., Boggs, E. M. & Aizenberg, J. Liquid-infused structured surfaces with exceptional anti-biofouling performance. *Proc Natl Acad Sci U S A* **109**, 13182–13187 (2012).

25. Kovalenko, Y. *et al.* Bacterial Interactions with Immobilized Liquid Layers. *Advanced Healthcare Materials* **6**, 1600948 (2017).

26. Juthani, N. *et al.* Infused polymers for cell sheet release. *Scientific Reports* **6**, (2016).

27. Shah, R. M., Cihanoğlu, A., Hardcastle, J., Howell, C. & Schiffman, J. D. Liquid-Infused Membranes Exhibit Stable Flux and Fouling Resistance. *ACS Applied Materials and Interfaces* **14**, 6148–6156 (2022).

28. Regan, D. P. & Howell, C. Droplet manipulation with bioinspired liquid-infused surfaces: A review of recent progress and potential for integrated detection. *Current Opinion in Colloid & Interface Science* **39**, 137–147 (2019).

29. Overton, J. C., Weigang, A. & Howell, C. Passive Flux Recovery in Protein-Fouled Liquid-Gated Membranes. *Article in Journal of Membrane Science* (2017) doi:10.1016/j.memsci.2017.06.019.

30. Sotiri, I., Overton, J. C., Waterhouse, A. & Howell, C. Immobilized liquid layers: A new approach to anti-adhesion surfaces for medical applications. *Experimental Biology and Medicine* **241**, 909–918 (2016).

31. Long, Y. *et al.* Slippery liquid-infused porous surface (SLIPS) with superior liquid repellency, anti-corrosion, anti-icing and intensified durability for protecting substrates. *Chemical Engineering Journal* **401**, 126137 (2020).

32. Bazyar, H. *et al.* On the Gating Mechanism of Slippery Liquid Infused Porous Membranes. *Advanced Materials Interfaces* **3**, 1600025 (2016).

33. Ngene, I. S., Lammertink, R. G. H., Wessling, M. & van der Meer, W. G. J. Particle deposition and biofilm formation on microstructured membranes. *Journal of Membrane Science* **364**, 43–51 (2010).

34. Polyvinylidene Flouride (PVDF) Membrane Filters, 0.45 Micron, 47m. https://www.sterlitech.com/polyvinylidene-flouride-pvdf-membrane-filters-0-45-micron-47mm-100-pk.html.

35. Wong, T. S. *et al.* Bioinspired self-repairing slippery surfaces with pressure-stable omniphobicity. *Nature* **477**, 443–448 (2011).

36. Krytox GPL 103 | PFPE Oil | Miller-Stephenson | Krytox Oils and Greases. https://miller-stephenson.com/product/krytox-gpl-103/.

37. Krytox GPL 107 | General Purpose Lubricants | Miller-Stephenson | Krytox. https://miller-stephenson.com/product/krytox-gpl-107/.

38. Herfst, S. *et al.* Drivers of airborne human-to-human pathogen transmission. *Current Opinion in Virology* **22**, 22–29 (2017).

39. Young, N. *et al.* International flight-related transmission of pandemic influenza A(H1N1)pdm09: an historical cohort study of the first identified cases in the United Kingdom. *Influenza and Other Respiratory Viruses* **8**, 66 (2014).

40. Country-to-Country Transfer of Patients and the Risk of Multi-Resistant Bacterial Infection on JSTOR. https://www-jstor-org.wv-o-ursus-proxy02.ursus.maine.edu/stable/23031002?pq-origsite=summon&seq=1.

41. Singer, D. A. Transmission of infections during commercial air travel. *The Lancet* **365**, 2176–2177 (2005).

42. Nasir, Z. A., Campos, L. C., Christie, N. & Colbeck, I. Airborne biological hazards and urban transport infrastructure: current challenges and future directions. *Environmental Science and Pollution Research* **23**, 15757–15766 (2016).

43. Regan, D. P. *et al.* Liquid-infused filters improve the recovery of captured airborne bacteria and viruses.

44. Verreault, D., Moineau, S. & Duchaine, C. Methods for Sampling of Airborne Viruses. *Microbiology and Molecular Biology Reviews : MMBR* **72**, 413 (2008).

45. Mainelis, G. Bioaerosol sampling: Classical approaches, advances, and perspectives. *https://doi-org.wv-o-ursus-proxy02.ursus.maine.edu/10.1080/02786826.2019.1671950* **54**, 496–519 (2019).

46. Pan, M., Lednicky, J. A. & Wu, C. Y. Collection, particle sizing and detection of airborne viruses. *Journal of Applied Microbiology* **127**, 1596–1611 (2019).

47. Cox, J., Mbareche, H., Lindsley, W. G. & Duchaine, C. Field sampling of indoor bioaerosols. *https://doi-org.wv-o-ursus-proxy02.ursus.maine.edu/10.1080/02786826.2019.1688759* **54**, 572–584 (2019).

48. Korves, T. M. *et al.* Bacterial communities in commercial aircraft high-efficiency particulate air (HEPA) filters assessed by PhyloChip analysis. *Indoor Air* **23**, 50–61 (2013).

49. "Handling and Manipulation of Water- and Air- Borne Biological Samples . . ." by Daniel P. Regan. https://digitalcommons.library.umaine.edu/etd/3353/.

50. Buck, R. C. *et al.* Perfluoroalkyl and polyfluoroalkyl substances in the environment: Terminology, classification, and origins. *Integrated Environmental Assessment and Management* **7**, 513–541 (2011).

51. Trier, X., Granby, K. & Christensen, J. H. Polyfluorinated surfactants (PFS) in paper and board coatings for food packaging. *Environmental Science and Pollution Research* **18**, 1108–1120 (2011).

52. Liu, Y., D'Agostino, L. A., Qu, G., Jiang, G. & Martin, J. W. High-resolution mass spectrometry (HRMS) methods for nontarget discovery and characterization of poly- and per-fluoroalkyl substances (PFASs) in environmental and human samples. *TrAC Trends in Analytical Chemistry* **121**, 115420 (2019).

53. Melo, T. M. *et al.* Ecotoxicological effects of per- and polyfluoroalkyl substances (PFAS) and of a new PFAS adsorbing organoclay to immobilize PFAS in soils on earthworms and plants. *Journal of Hazardous Materials* **433**, 128771 (2022).

54. Nelson, B. & Kaminsky, D. B. A growing drive to get rid of cancer-linked "forever chemicals." *Cancer Cytopathology* **129**, 7–8 (2021).

55. Costello, M. C. S. & Lee, L. S. Sources, Fate, and Plant Uptake in Agricultural Systems of Per- and Polyfluoroalkyl Substances. *Current Pollution Reports* 1–21 (2020) doi:10.1007/S40726-020-00168-Y/TABLES/2.

56. Abunada, Z., Alazaiza, M. Y. D. & Bashir, M. J. K. An Overview of Per- and Polyfluoroalkyl Substances (PFAS) in the Environment: Source, Fate, Risk and Regulations. *Water 2020, Vol. 12, Page 3590* **12**, 3590 (2020).

57. Mora, A. M. *et al.* Prenatal exposure to Perfluoroalkyl substances and adiposity in early and mid-childhood. *Environmental Health Perspectives* **125**, 467–473 (2017).

58. Shahsavari, E. *et al.* Challenges and Current Status of the Biological Treatment of PFAS-Contaminated Soils. *Frontiers in Bioengineering and Biotechnology* **8**, 1493 (2021).

59. Kang, H., Zhao, B., Li, L. & Zhang, J. Durable superhydrophobic glass wool@polydopamine@PDMS for highly efficient oil/water separation. *Journal of Colloid and Interface Science* **544**, 257–265 (2019).

60. Sun, W. *et al.* Fabrication of polydimethylsiloxane-derived superhydrophobic surface on aluminium via chemical vapour deposition technique for corrosion protection. *Corrosion Science* **128**, 176–185 (2017).

61. Cellulose filter papers | Cytiva. https://www.cytivalifesciences.com/en/us/shop/whatman-laboratory-filtration/cellulose-filter-papers.

62. Contact Angle. https://imagej.nih.gov/ij/plugins/contact-angle.html.

BIOGRAPHY OF AUTHOR

Justin Hardcastle was born March 14th, 1998 in Danbury, Connecticut. He was raised in Galway, New York and graduated from Galway High School as Salutatorian in 2016. He attended the University of New Hampshire and graduated in 2020 with a Bachelor's degree in Bioengineering. There, he was an active member of the UNH Woodsmen Team, and became the Northeast Qualifier Winner for the Stihl Collegiate Series and competed at the Stihl Collegiate National Championship in 2019. He began attending the University of Maine in the fall of 2020 as a member of the Biomedical Engineering graduate program. After receiving his degree, Justin will be joining PerkinElmer as a Senior Research Specialist in Cell Culture. Justin is a candidate for the Master of Science degree in Biomedical Engineering from the University of Maine in August 2022.